BIOCHEMISTRY
including biophysical chemistry & molecular biology

Article

pubs.acs.org/biochemistry

The Hepatitis B Virus Core Protein Intradimer Interface Modulates Capsid Assembly and Stability

Lisa Selzer,[†] Sarah P. Katen,[†,§] and Adam Zlotnick*[,†,‡]

[†]Department of Molecular and Cellular Biochemistry, Indiana University, Bloomington, Indiana 47405, United States
[‡]Department of Biology and Department of Chemistry, Indiana University, Bloomington, Indiana 47405, United States

Supporting Information

ABSTRACT: During the hepatitis B virus (HBV) life cycle, capsid assembly and disassembly must ensure correct packaging and release of the viral genome. Here we show that changes in the dynamics of the core protein play an important role in regulating these processes. The HBV capsid assembles from 120 copies of the core protein homodimer. Each monomer contains a conserved cysteine at position 61 that can form an intradimer disulfide that we use as a marker for dimer conformational states. We show that dimers in the context of capsids form intradimer disulfides relatively rapidly. Surprisingly, compared to reduced dimers, fully oxidized dimers assembled slower and into capsids that were morphologically similar but less stable. We hypothesize that oxidized protein adopts a geometry (or constellation of geometries) that is unfavorable for capsid assembly, resulting in weaker dimer−dimer interactions as well as slower assembly kinetics. Our results suggest that structural flexibility at the core protein intradimer interface is essential for regulating capsid assembly and stability. We further suggest that capsid destabilization by the C61−C61 disulfide has a regulatory function to support capsid disassembly and release of the viral genome.

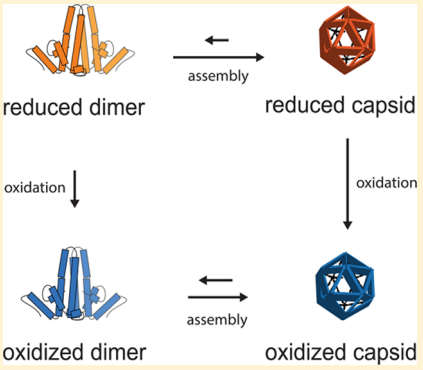

Icosahedral virus capsid assembly is a highly regulated, efficient process in which tens to hundreds of capsid proteins form a stable virus shell. During the virus life cycle, capsid assembly has to be regulated to ensure correct packaging and release of the viral genome. Newly formed capsids must be stable to withstand the extracellular environment. Capsids also must be unstable enough to allow disassembly, to release the viral genome.

One mechanism regulating virus capsid assembly is allosteric activation, described as dynamic or conformational changes that switch the capsid protein from assembly inactive to assembly active states. Allosteric changes during assembly help to package the right nucleic acid to define the nucleation step and contribute to an induced fit mechanism for elongation. Nucleation and induced fit both minimize the accumulation of intermediates.[1−3]

Allosteric regulation, mediated by binding of nucleic acid to the capsid protein, has been observed in retroviruses and bacteriophage MS2.[2,4,5] Also, extensive studies of the hepatitis B virus (HBV) capsid protein indicate allosteric changes during assembly, independent of nucleic acid binding. Assembly studies show that zinc ions induce a conformational change to the HBV capsid protein dimer that alters its assembly behavior.[6] Additionally, X-ray crystallography revealed structural differences between free HBV dimers and dimers in capsids.[7,8]

The HBV capsid is formed from 120 core protein homodimers that are arranged with T = 4 icosahedral symmetry. A small portion of the HBV capsids have T = 3 icosahedral symmetry and consist of 90 homodimers.[9] The full-length core protein has 183 amino acids and is comprised of an assembly domain (amino acids 1−149) and a nucleic acid-binding domain (amino acids 150−183).[10] The assembly domain, termed Cp149 in this paper, can be expressed in *Escherichia coli* and assembles spontaneously in response to an increase in ionic strength.[11] Cp149 thereby forms particles that are morphologically indistinguishable from capsids isolated from cell cultures.[12,13]

In vitro capsid assembly of HBV has been well-characterized. Simulations and light scattering experiments have shown that the assembly of large populations of particles displays sigmoidal kinetics.[14−16] Assembly for each capsid starts with nucleation that is followed by elongation and growth involving the addition of free dimer subunits. Because observations of *in vitro* assembly reactions typically are based on very large ensembles of molecules, interpretation of assembly kinetics requires particular care. For example, the initial lag phase during assembly kinetics is the time to establish a steady stream of intermediates.[15,16]

HBV capsid assembly is defined by multiple weak interdimer contact energies [approximately 3−5 kcal/mol (5−8 kT)]. However, a T = 4 HBV capsid has 240 interdimer contacts. In comparison, association energies found in antibody−protein

Received: June 11, 2014
Revised: August 5, 2014
Published: August 7, 2014

   dx.doi.org/10.1021/bi500732b | *Biochemistry* 2014, 53, 5496−5504

a

```
                    40        50        60        70        80        90        100       110
Human genotype A:   EALESPEHCSPHHTALRQAILCWGELMNLATWVGGNLEDPASRELVVSYVNVNMGLKLRQILWFHISCLTFGRE
Human genotype B:   EALESPEHCSPHHTALRQAILCWGELMNLATWVGSNLEDPASRELVVSYVNVNMGLKIRQLLWFHISCLTFGRE
Human genotype C:   DALESPEHCTPHHTALRHVCLCWGDLMNLATWVGTNLEDQASRDLVVSYVNTNMGLKFRQLLWFHISCLTFGRD
Human genotype D:   DALESPEHCTPNHTALRQAILCWGELMTLASWVGNNLEDPAARDLVVNYVNTNMGLKIRQLLWFHISCLTFGRE
Human genotype F:   DALESPEHCTPNHTALRQAILCWGELMTLASWVGNNLEDPAARDLVVNYVNTNMGLKIRQLLWFHISCLTFGRD
Human genotype G:   EALESPEHCSPNHTALRQAILCWGELMTLASWVGNNLEDPASREQVVNYVNTNMGLKIRQLLWFHISCLTFGRE
Human genotype H:   ESLESSDHCSPHHTALRQAILCWGELMTLATWVGNNLEDPASRDLVVNYVNTNMGLKIRQLLWFHISCLTFGRE
Woolly Monkey:      EALESPEHCSPHHTALRETILCWGELMTLATWVGNNLEDPASRDLVVNYVNTNMGLKIRQLLWFHISCLTFGRE
Ground Squirrel:    EALESSDHCSPHHTALRQTVLCWGELMSLASWVGTNLEDPAARELVVSYVNDNMGLKVRQLLWFHLSCLTFGRE
Woodchuck:          EELTGREHCSPHHTAIRQALVCWEELTRLIAWMSANINSEEVRRVIVAHVNDTWGLKVRQNLWFHLSCLTFGQH
Chimpanzee:         EELTGREHCSPHHTAIRQALVCWDELTKLIAWMSSNITSEQVRTIIVNHVNDTWGLKVRQSLWFHLSCLTFGQH
```

b

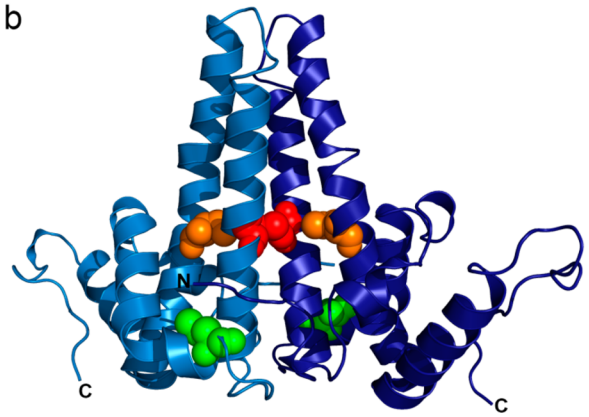

Figure 1. (a) Sequence alignment of HBV core protein sequences from human HBV genotypes (A−D and F−H) and hepadnaviruses isolated from naturally infected ground squirrel, woodchuck, woolly monkey, and chimpanzee. Residue C61 is completely conserved. (b) Ribbon representation of the Cp149 dimer (Protein Data Bank entry 1QGT). Monomers are colored light and dark blue. Residues C61 (red), I97 (orange), and L42 (green) are shown as spheres. C61 forms a disulfide across the intradimer interface.

interactions were approximately 11−15 kcal/mol or 15−25 kT.[17,18]

In this study, we investigated how changes at the intradimer interface, the monomer−monomer contact region, propagate to the interdimer interface to influence HBV core protein assembly and capsid stability. We utilized a pair of cysteine residues located at position 61 that can form an intradimer disulfide bond. Cysteine 61 is conserved throughout all mammalian HBV core proteins (Figure 1). The C61−C61 disulfide has been shown to form within HBV particles assembled from full-length core protein expressed in *E. coli*.[19,20] However, recent reports found no disulfide in freshly purified RNA-filled capsids, indicating oxidation of capsids formed by full-length protein might be slower than that in empty capsids formed by Cp149, and there are no data for mature DNA-filled capsids.[21] We observed that formation of the C61−C61 disulfide bond alters capsid assembly and stability. Free dimers oxidized slowly compared to dimer within capsid, which led us to hypothesize that the oxidized form would favor capsid assembly. However, oxidized Cp149 dimers assemble slowly to form capsids that are less stable than reduced capsids. We thereby show that changes at the intradimer interface are an important regulator of assembly. However, our results also suggest that disulfide bond formation during the HBV life cycle may promote the disassembly required to release the viral genetic material.

MATERIALS AND METHODS

Sequence Alignment. Sequences obtained from the National Center for Biotechnology Information (NCBI) Protein Data Bank were aligned using CLUSTAWL.

Cp149red Sample Preparation. Cp149 was expressed in *E. coli* using a pET11-based vector. Cp149 dimers were purified as previously described.[22] Aliquots of frozen Cp149 were dialyzed into 50 mM HEPES (pH 7.5) prior to use.

Oxidation Rate of Dimer and Capsid. Cp149red (50 μM) was incubated with and without the addition of 300 mM NaCl at 37 °C for up to 7 days. Capsid and dimer fractions were incubated with 250 mM iodoacetamide to block free thiols. Dimers containing the C61−C61 disulfide bond were separated from monomers using nonreducing SDS−PAGE.

Oxidation of Cp149 Dimer and Re-reduction. Cp149red (50 μM) was assembled by addition of 200 mM NaCl and incubation at 37 °C until capsids were fully oxidized. Capsids were purified by size-exclusion chromatography (SEC) and disassembled by addition of 3 M urea for 1.5 h at 4 °C. Oxidized dimers were dialyzed into 50 mM HEPES (pH 7.5) for further experiments. For re-reduction, 10 μM Cp149ox was incubated with 400 mM DTT at 4 °C for 24 h and dialyzed for 2 h into 50 mM HEPES (pH 7.5) to remove excess DTT. The oxidation state of the re-reduced Cp149 was determined using nonreducing SDS−PAGE.

Size-Exclusion Chromatography (SEC). SEC experiments were performed using a 10/300 Superose 6 column (GE Healthcare) mounted on an HPLC system (Shimadzu) with a temperature-controlled autosampler. For thermodynamic experiments, varying concentrations of Cp149ox were assembled by addition of NaCl (to a final concentration of 300 mM) at 23−40 °C for 24 h. Dimer and capsid fractions were separated and quantified by SEC using 50 mM HEPES (pH 7.5) and 300 mM NaCl as elution buffer. Long-term kinetic experiments were conducted at 23 °C. Assembly of 1.8 mL of 7

dx.doi.org/10.1021/bi500732b | *Biochemistry* 2014, 53, 5496−5504

μM Cp149red, Cp149ox, Cp149-C61S, and re-reduced Cp149ox protein was initiated by the addition of 300 mM NaCl. Samples were analyzed hourly by SEC using 50 mM HEPES (pH 7.5) and 300 mM NaCl as elution buffer. The concentrations of dimer and capsid fractions for all assembly reactions were determined by integrating the area under the dimer and capsid peaks, determined by SEC. The area of the peaks could then be compared to the initial protein concentration.

Analysis of Thermodynamic Data. Thermodynamic analysis was performed as described in detail in ref 17.

Sucrose Gradient Centrifugation. Capsid assembly of 30 μM Cp149red or Cp149ox was induced by the addition of 300 mM NaCl and the sample incubated for 24 h at 23 °C; 300 μL of the assembly reaction mixture was loaded onto a 10 to 40% (w/v) continuous sucrose gradient and centrifuged for 4 h at 20 °C and 200000*g*.

Transmission Electron Microscopy. Samples extracted from sucrose gradients were applied to glow-discharged carbon copper grids and stained with 2% uranyl acetate. Micrographs were recorded at a nominal magnification of 25000× using a JEOL-1010 transmission electron microscope equipped with a 4K × 4K charge-coupled device (CCD) camera.

Light Scattering Experiments. Light scattering experiments were performed using a stopped-flow spectrometer (KinTek SF-300X). Scattered light was detected at 90° using an excitation wavelength of 320 nm. Assembly of increasing concentrations of Cp149red and Cp149ox was initiated at 37 °C by addition of NaCl to a final concentration at 600 mM.

Lag times were determined as described by Hagan et al.[23] The elongation rate constant was calculated using eq 1, adapted from ref 23, under the assumption $fc_0 \gg b_{elong}$.

$$t_{lag} \approx t_{elong} \approx n_{elong}/fc_0 \quad (1)$$

where f is the elongation rate constant, c_0 is the total protein concentration, b_{elong} is the dissociation rate constant, t_{lag} is the lag time, t_{elong} is the mean elongation time, and n_{elong} is the number of steps to complete a nucleated capsid. For 120 dimer HBV with a three-dimer nucleus, n_{elong} = 117.

Urea Disassembly. Capsid assembly of varying percentages of Cp149-C61S and Cp149ox at a total concentration of 20 μM was initiated by the addition of 300 mM NaCl and the sample equilibrated for 24 h at 23 °C. Prior to dissociation, capsids were purified using SEC. To 2.5 μM capsid, measured in dimer concentration, urea was added to a final concentration of 0−4 M. Disassembly was analyzed by SEC. Urea was freshly prepared in 50 mM Tris-HCl (pH 7.5) and 300 mM NaCl to scavenge cyanide from decomposing urea.[24]

RESULTS

Dimer within Capsid Oxidizes Relatively Rapidly. Disulfide bond stability in proteins is highly dependent on the conformation and environment of the cysteine residues. The intradimer interface of the HBV dimer displays significant structural differences between free dimers and dimers within capsids.[7,8,25] It is therefore a marker of structural and dynamic changes of the intradimer interface.

An indication of the propensity of the C61−C61 disulfide to oxidize was the rate of disulfide bond formation. The oxidation rates of Cp149 dimer and capsid were measured by incubating samples for various times, quenching aliquots with iodoacetamide, and separating disulfide-cross-linked dimers from monomers by nonreducing SDS−PAGE. Iodoacetamide covalently reacts with cysteines to block further disulfide bond formation. Oxidized Cp149 dimer and iodoacetamide-passivated monomer were observed as bands with molecular masses of 34 and 17 kDa, respectively. Our kinetic data fit the expected first-order rate law. For capsids, the $t_{1/2}$ of oxidation was 53 h (Figure 2a). Free dimers, however, oxidized ∼7 times slower with an oxidation half-life of 392 h. This suggests that dimers within capsids adopt a conformation that favors the formation of a disulfide bond. On the basis of this observation, we developed a working hypothesis that oxidized dimer represents an assembly active conformation that would assemble into stable capsids more readily than reduced dimer.

Efforts to measure stability of the C61−C61 disulfide bond in capsid and free dimer by equilibration at a given redox potential or by measuring the rate of reduction were frustrated.[26] Even with extremely high concentrations of up to 1 M β-mercaptoethanol, glutathione, or tris(2-carboxyethyl)-phosphine, little to no reduction of oxidized Cp149 was observed. The addition of 400 mM dithiothreitol (DTT) led to an approximately 20% reduction of Cp149 after incubation for 48 h (Figure 2b, inset, right lane). The limited reduction may be related to the limited accessibility of the disulfide bond to reducing agents, the intrinsic stability of the disulfide to a given redox potential,[26] and the fact that DTT itself was subject to air oxidation under the conditions used in this experiment.

Oxidized Dimer Assembled into Small Amounts of Capsids. To test the hypothesis that the C61−C61 disulfide locked the dimer in an assembly active state, we investigated the assembly behavior of oxidized protein. Freshly purified Cp149, here called Cp149red (Figure 2b, inset, left lane), is mainly in the reduced form, lacking the intradimer C61−C61 disulfide. To generate fully oxidized dimer, Cp149 was assembled into capsids and incubated until the C61 cysteines were fully oxidized. Capsids were then disassembled to obtain fully oxidized Cp149 dimers, here called Cp149ox (Figure 2b, inset, middle lane). An important control for these experiments was Cp149-C61S, a mutant dimer that lacks the C61 cysteines and thus resembles dimer that is 100% reduced.

On the basis of the facility of C61−C61 disulfide formation in capsids, we predicted that Cp149ox would assemble faster and yield more capsid than Cp149red. However, results from assembly studies ran contrary to this prediction. We investigated the long-term kinetics of Cp149ox, in 1 h increments, over 24 h at 23 °C (Figure 2b). At most, 2% of the 7 μM Cp149ox dimer assembled into capsids. In comparison, 7 μM Cp149red yielded ∼33% capsid, while Cp149-C61S assembled at an intermediate rate and yielded 16% capsids.

Capsid assembly can be described with good approximation by the law of mass action. When the free dimer concentration is increased during assembly, little to no capsid assembly is observed until the total dimer concentration exceeds a pseudocritical concentration.[16] Above this pseudocritical concentration, almost all additional free dimer assembled into capsid, leaving a nearly constant concentration of free dimer (Figure 3a). The pseudocritical concentration can be estimated from the amounts of assembled capsid and the corresponding amounts of free dimer at the 21 h time point. At 23 °C and 300 mM NaCl, these values are 4.7 μM Cp149red and 5.9 μM Cp149-C61S. At an initial protein concentration of 7 μM, Cp149ox was below its pseudocritical concentration, resulting in extremely small amounts of assembled capsids (Figure 2b).

dx.doi.org/10.1021/bi500732b | *Biochemistry* 2014, 53, 5496−5504

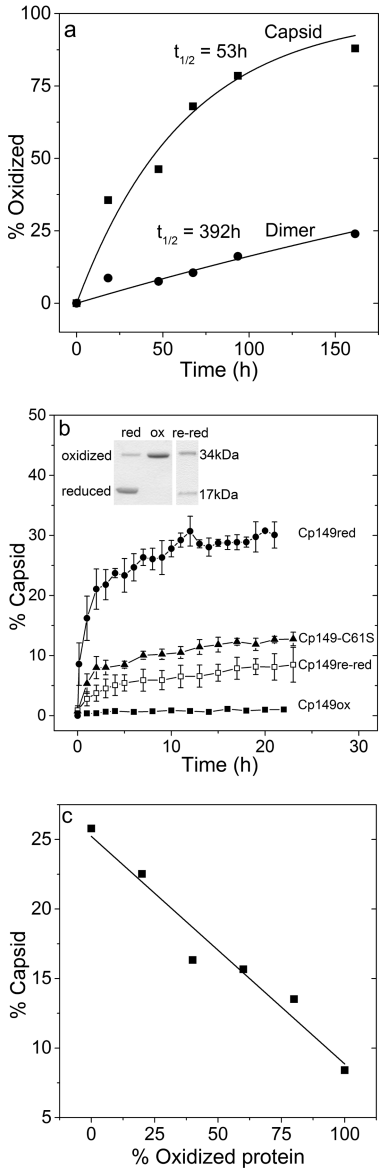

Figure 2. Oxidation paradox, in which capsids favor disulfide formation, whereas the disulfide disfavors capsid assembly. (a) Representative experiment showing the oxidation rates of free dimer and capsids at 37 °C. The C61−C61 disulfide bond formed 7.4 times faster in Cp149 dimers within capsids than in free Cp149 dimers. Oxidation states of Cp149 capsid dimer were determined by nonreducing SDS−PAGE (panel b inset). Data were fit to a first-order rate law. A baseline level of ∼5% oxidation in dimer and capsid fractions was adjusted to zero to ensure accurate curve fitting. (b) Assembly of capsids, quantified by SEC at 23 °C, was monitored over a 24 h time period. Cp149ox assembled into less capsid than Cp149red. Samples of reduced Cp149 (Cp149red), fully oxidized Cp149 (Cp149ox), Cp149 with C61 mutated to serine (Cp149-C61S), and partially re-reduced Cp149 (Cp149re-red) were at a dimer concentration of 7 μM. The inset shows nonreducing SDS−PAGE of Cp149red (red), Cp149ox (ox), and Cp149re-red (re-red). (c) Representative series of co-assembly reactions of Cp149-C61S with varying percentages of Cp149ox were quantified by SEC at 23 °C. Oxidized protein decreased the yield of capsid. The total dimer concentration was 10 μM. Assembly for panels b and c was induced by 300 mM NaCl at 23 °C.

We hypothesize that these differences in assembly can be attributed to changes at the intradimer interface that are located

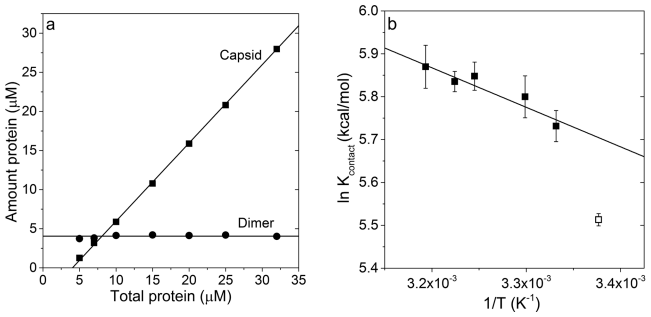

Figure 3. Assembly of Cp149ox displays a dimer−dimer contact energy that is weaker than that of Cp149red. (a) Assembly under equilibrium conditions that included increasing concentrations of Cp149ox was induced by addition of 300 mM NaCl at 37 °C. A pseudocritical concentration of 4.0 ± 0.2 μM was observed. Dimer and capsid fractions were quantified by SEC and plotted as dimer concentration. (b) van't Hoff plot for the assembly of Cp149ox. The ln $K_{contact}$ for 23 °C (□) was excluded from analysis of the van't Hoff plot because the assembly reaction of Cp149ox was not fully equilibrated at this temperature.

around residue 61. Upon comparison of C61S and Cp149red, replacement of cysteine with the more hydrophilic serine very likely perturbs some interactions at the intradimer interface. Similarly, oxidation of the C61−C61 disulfide decreases the degree of freedom of the intradimer interface. Similar effects have been observed upon mutation of residue F97 (strain ayw, adyw) or I97 (strain adr, adw) (Figure 1b) to leucine. Mutation of F97 or I97 to leucine causes secretion of mainly immature virions in cell culture and resulted in increased assembly kinetics *in vitro*.[27−29]

We confirmed that assembly activity of Cp149ox could be restored by re-reduction of Cp149ox. Only ∼20% of Cp149ox could be reduced in the presence of high concentrations of reducing DTT after incubation for 48 h (Figure 2b, inset, right lane). Partial re-reduction partially restored assembly of Cp149ox (Figure 2b). Re-reduced dimer assembled into a total of 7% capsid over the experimental time period, indicating that the pseudocritical concentration of assembly had decreased to 6.5 μM.

To further evaluate the assembly of Cp149ox, we tested co-assembly of Cp149ox with Cp149-C61S. We assembled increasing concentrations of Cp149ox with Cp149-C61S at room temperature for at least 24 h to approach equilibrium. Co-assembly of Cp149ox with Cp149-C61S decreased the yield of capsid in a dose-dependent manner (Figure 2c). These results indicated that Cp149ox does not, as suggested by the propensity of capsids to enhance oxidation, promote capsid formation but is unfavorable for capsid assembly.

Cp149ox Displays a Weaker Dimer−Dimer Contact Energy Than Cp149red. To quantify the assembly properties of Cp149ox and define the basis of the decreased level of assembly, we determined the thermodynamics of Cp149ox assembly under equilibrium conditions. Shown in Figure 3a are the 24 h concentrations for capsid and dimer in terms of dimer concentrations for assembly reactions at 37 °C.

As described above, capsid assembly starts when the free dimer concentration exceeds a pseudocritical concentration, also known as K_{Dapp}, the apparent dissociation constant. K_{Dapp} is evident as the concentration of free dimer and also as the *x*-intercept of the capsid concentration. During assembly of increasing concentrations of dimer, the free/unassembled

dx.doi.org/10.1021/bi500732b | *Biochemistry* 2014, 53, 5496−5504

dimer concentrations fit a linear regression with a slope of zero, indicating the assembly reaction of Cp149ox was very close to equilibrium within 24 h (Figure 3a).[30]

The observed K_{Dapp} of Cp149ox at 300 mM NaCl and 37 °C was 4.0 ± 0.2 μM, which is significantly higher than the K_{Dapp} for Cp149red of 1.4 μM determined under the same assembly conditions.[17] Thus, Cp149ox forms dimer−dimer interactions weaker than those of Cp149red at 37 °C. To define the enthalpy, ΔH, and entropy, ΔS, of the pairwise dimer−dimer contact energy, $\Delta G_{contact}$, we used a van't Hoff analysis (Figure 3b). The nearly linear temperature dependence seen in the van't Hoff plot indicates that heat capacity-dependent curvature is near zero. We therefore fit the data to a straight line and estimated the enthalpy as a temperature-independent value.

The thermodynamic parameters of assembly for Cp149ox differed markedly from those of Cp149red. Cp149ox, at 37 °C, had a markedly weaker $\Delta G_{contact}$ of −3.6 ± 0.01 kcal/mol compared to that of Cp149red (−4.1 kcal/mol) (Table 1).[17] In

Table 1. Thermodynamic Parameters of Cp149ox and Cp149red Assembly at 300 mM NaCl and 37 °C[a]

	Cp149ox	Cp149red
ΔH (kcal/mol)	1.8	4.3
ΔS (cal mol^{-1} K^{-1})	17.5	27
ΔST (kcal/mol)	5.4	8.4 ± 0.6
ΔG (kcal/mol)	−3.6 ± 0.01	−4.1
K_{Dapp} (μM) at 37 °C	4 ± 0.2	1.4

[a]For Cp149red, values of ΔH and ΔS were taken from Table 1 of ref 17 and ΔG was calculated from ΔH and ΔS.

virus capsids, even small changes in $\Delta G_{contact}$ can drastically change the overall capsid stability because of the large number of pairwise subunit interactions within a capsid, 240 of them for HBV. Our calculations for $\Delta G_{contact}$ are based on the formation of only T = 4 particles. Accounting for the varying percentage of T = 3 particles changes $\Delta G_{contact}$ by <0.01 kcal/mol, which is below the error of our measurements. Cp149ox and Cp149red showed strikingly different compensating changes in the values for the enthalpy and entropy of assembly. ΔH and ΔS for assembly of Cp149ox were 1.8 kcal/mol and 17.5 cal mol^{-1} K^{-1}, respectively. In comparison, Cp149red had a ΔH of 4.3 kcal/mol and a ΔS of 27 cal mol^{-1} K^{-1} (from ref 17) (Table 1).

For both reduced and oxidized Cp149, HBV capsid assembly is an entropically driven process.[17] If assembly were based on rigid subunits associating, values of ΔH and ΔS would be expected to correlate with the amount of buried hydrophobic surface area and the amount of replaced bulk water. However, capsids of both Cp149ox and Cp149red have similar morphologies and thus similar amounts of buried interdimer surface. Therefore, the large differences in the values of enthalpy and entropy for Cp149red and Cp149ox must be related, at least in part, to the conformational changes in the free dimer constrained by the C61−C61 disulfide. These observations agree with the data in Figure 2c showing Cp149ox formed small amounts of capsid and inhibited capsid assembly during co-assembly with Cp149-C61S.

Cp149ox Favors the Formation of T = 3 Particles. To further investigate how changes at the intradimer interface affect assembly, we investigated the morphology of the assembly products of Cp149ox. We subjected assembly reactions of Cp149ox and Cp149red to sucrose gradient centrifugation. Cp149ox assembled into ∼40% more T = 3 particles than Cp149red (Figure 4a). In contrast, approximately 90−95% of Cp149red capsids had a T = 4 morphology.

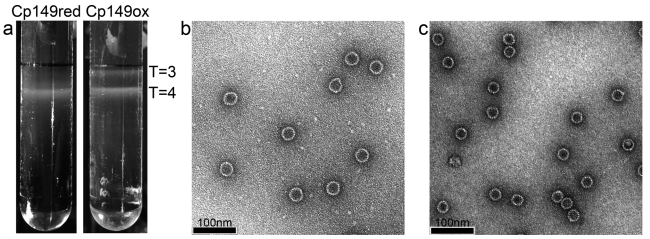

Figure 4. Oxidation changed the relative proportion of T = 3 capsids. (a) Sucrose gradient centrifugation showed Cp149ox assembled into a proportion of T = 3 particles higher than that of Cp149red. (b) Negatively stained electron micrograph of T = 4 sized particles, with a diameter of 30 nm[13] extracted from the lower band of the Cp149ox sucrose gradient. (c) Negatively stained electron micrograph of T = 3 particles, displaying a diameter of 26 nm[13] extracted from the upper band of the Cp149ox sucrose gradient.

Notably, there was no evidence of intermediates or misassembled complexes in either assembly reaction mixture, which would show up as cloudiness in the gradient. The absence of intermediates was also confirmed by SEC, where the capsid peak migrated after the void volume. In comparison, large amounts of intermediates can be observed during drug-induced kinetic traps.[31] Particles extracted from the upper and lower bands of the sucrose gradient were investigated by TEM and had diameters of 26 and 30 nm, respectively (Figure 4b,c). These capsids were indistinguishable from particles formed by Cp149red previously investigated.[13]

These results indicated that the oxidation state of the dimer affects the quaternary structure of the capsids. We can thereby assume that formation of the disulfide affects the geometry of the dimer molecule, disfavoring capsid formation overall but increasing the relative preference for T = 3 capsids (this latter point may have its basis in kinetics or thermodynamics).

Cp149ox Assembles More Slowly Than Cp149red. To provide a complete picture of how C61 oxidation affects the energetics of capsid assembly, we investigated the assembly kinetics of Cp149ox. In particular, a difference in elongation rates would indicate whether Cp149red and Cp149ox had to overcome different energetic barriers to participate in assembly. As assembly reactions of Cp149ox did not produce large fractions of intermediates (Figure 4), the light scattering signal corresponds well to the amount of capsid formed in solution. Interpretation of the kinetics for assembly of a large number of capsids is distinctly different from interpretation of kinetics for forming a single crystal.[16] For capsid assembly, the lag phase corresponds to formation of a steady state of intermediates from which we can estimate the average rate for elongation steps.[16]

We chose assembly conditions that included a high salt concentration (600 mM NaCl) and an increased temperature (37 °C) to facilitate comparison of the Cp149ox and Cp149red assembly reactions. At corresponding initial protein concentrations, Cp149ox yielded only ∼40% the amount of capsid that Cp149red formed (Figure 5a,b). The early time points of the assembly kinetics revealed a significant difference in the duration of the lag phases between Cp149ox and Cp149red. As described by Hagan et al., the lag time of an assembly reaction can be directly related to the time to complete an individual capsid.[23] From this information, we can estimate the

dx.doi.org/10.1021/bi500732b | Biochemistry 2014, 53, 5496−5504

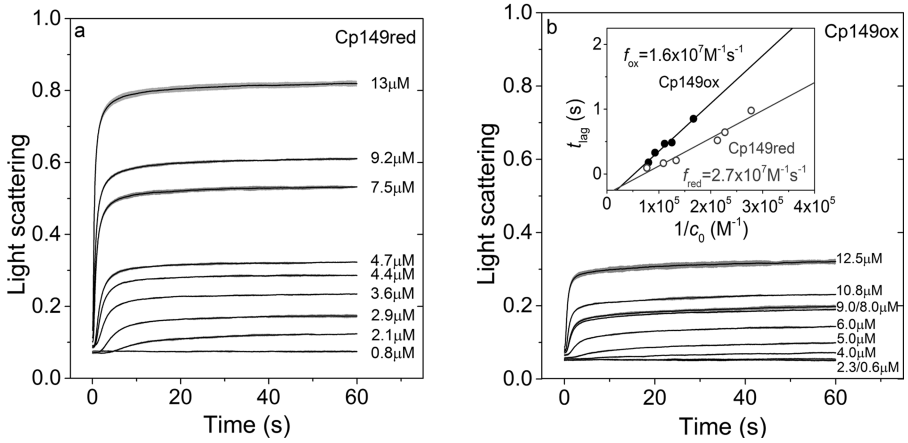

Figure 5. Light scattering of assembly reactions showed Cp149ox assembled slower and into less capsid than Cp149red. Increasing concentrations of (a) Cp149red and (b) Cp149ox were induced to assemble with NaCl at a final concentration of 600 mM at 37 °C. Assembly traces are averages of three experiments. Total protein concentrations are noted at the right end of assembly traces. The inset shows lag times of the assembly reactions, determined from light scattering traces, for Cp149red and Cp149ox, plotted vs the inverse of the total protein concentration.

average rate for the elongation steps. We measured the lag times, as described by Hagan et al., by extrapolating the steepest part of the assembly curve to the baseline using a linear regression. To work with the best signal, we only used the lag phases for reactions of 6−12.5 μM Cp149ox and 3.6−13 μM Cp149red. Lag times were plotted against the inverse of the total protein concentration to obtain the elongation rate constants (eq 1) (Figure 5b, inset). To simplify our calculations, we assumed that Cp149red and Cp149ox assembled entirely into T = 4 particles. Performing the calculation for the formation of only T = 3 particles only slightly changed the value for the elongation rate. The calculated elongation rate constants revealed that Cp149ox assembled 1.7 times slower than Cp149red (Figure 5b, inset).

Capsids from Cp149ox Are Less Stable to Treatment with Urea Than Capsids from Reduced Dimer. To confirm the observation based on assembly that Cp149ox capsids were less stable than capsids from Cp149red, we investigated capsid stability by urea-induced disassembly. Urea can induce HBV capsid dissociation without dimer unfolding.[17] Importantly, urea does not affect ionic strength, which modulates capsid stability. Capsids assembled from Cp149ox and Cp149-C61S were incubated for 24 h with varying concentrations of urea and the disassembly products analyzed by SEC. The disassembly curves displayed a sigmoidal shape consistent with a two-state reaction (Figure 6) as described previously.[32] Capsids formed entirely by Cp149-C61S appeared to be the most stable. HBV displays a large hysteresis to disassembly.[32] We therefore did not quantify the free dimer−dimer contact energy from disassembly experiments. To ensure that Cp149 dimers did not become irreversibly denatured during their exposure to urea, we monitored intrinsic fluorescence over time and at different urea concentrations. Folded dimer has a characteristic blue-shifted tryptophan emission at 323 nm. Dimer unfolding results in an increased fluorescence intensity and a red shift to ~345 nm.[32] Even at 3.8 M urea, no such change in fluorescence was apparent for Cp149 and Cp149-C61S (Figure 1 of the Supporting Information).

A clear shift of the disassembly transition toward lower urea concentrations was observed for capsids containing increasing mole fractions of Cp149ox, showing oxidized capsids were less stable to urea dissociation.

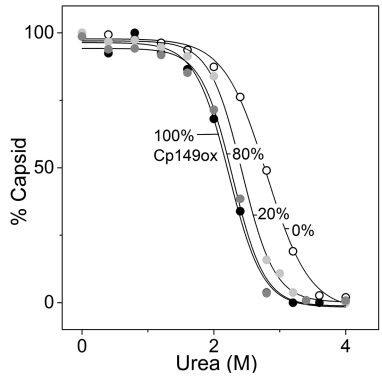

Figure 6. Capsids assembled from increasing amounts of oxidized protein showed decreased stability to urea. Capsids were assembled from 100% Cp149ox (black circles), a mixture of 80% Cp149ox and 20% Cp149-C61S (dark gray circles), a mixture of 20% Cp149ox and 80% Cp149-C61S (light gray circles), or 100% Cp149-C61S (white circles). The fitted lines were calculated for unimolecular transitions and were plotted to guide the eye.

■ DISCUSSION

We have shown that dimers within capsids adopt a conformation (or family of conformations) that favors C61−C61 disulfide formation (Figure 2a). Compared to free Cp149 dimers, dimers within capsids oxidized faster, indicating that structural and/or dynamic changes at the intradimer interface favor disulfide formation. Our results stand in agreement with findings from crystallographic studies showing structural differences at the intradimer interface between free dimers and dimers within capsids.[7,8] The main structural differences between free dimers and dimers within capsids lay in the spike tips and the dimer contact domain, indicating the dimer interface plays an important role in propagating structural changes through the dimer molecule.[7]

Even though dimers within capsids favor disulfide formation, capsids of oxidized dimers are not as stable as capsids of reduced dimers, summarized in Figure 7a. The core protein is a dynamic molecule that is able to access assembly active and inactive conformations in its free unbound form. We suggest that during assembly this equilibrium of states shifts, favoring assembly active conformations that facilitate dimer−dimer

dx.doi.org/10.1021/bi500732b | Biochemistry 2014, 53, 5496−5504

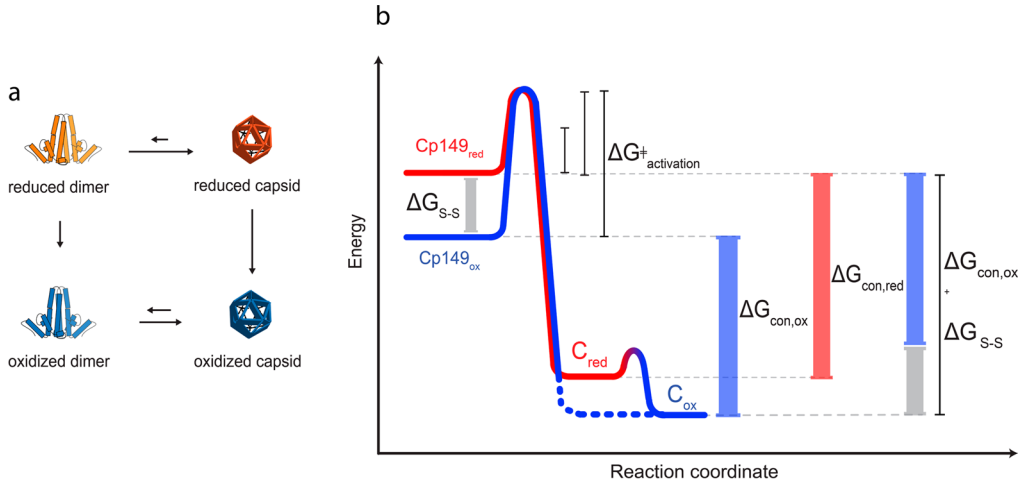

Figure 7. Redox state of the C61−C61 disulfide influences the kinetics and thermodynamics of capsid assembly. (a) Capsids oxidize faster than free dimers; these reactions are essentially unidirectional. Oxidized protein assembles slower than reduced protein to form capsids that are less stable. Thus, the model of assembly of reduced and oxidized dimer is based on kinetic and thermodynamic results. Long arrows indicate energetically favored and short arrows energetically unfavored reactions. (b) Energy diagram visualizing the thermodynamic and kinetic properties of Cp149ox (blue) and Cp149red (red) assembly. Because of the structural constraints, oxidized protein (Cp149ox) has to overcome an activation energy barrier ($\Delta G^{\ddagger}_{activation}$) higher than that of reduced dimer (Cp149red), resulting in slower assembly kinetics for Cp149ox. Cp149ox has a dimer−dimer contact energy ($\Delta G_{con,ox}$) weaker than that of Cp149red ($\Delta G_{con,red}$), thereby forming capsids that are less stable than those of Cp149red. Even though reduced capsids are overall more stable than oxidized capsids, formation of the C61−C61 disulfide bond is energetically favored. The disulfide bond formation causes a decrease in the dimer−dimer contact energy creating an overall metastable oxidized capsid ($\Delta G_{con,ox}$ + ΔG_{S-S}). The energy term ΔG_{S-S} includes contributions from dimer interactions and disulfide formation.

interactions (Figure 7b). During this process, structural changes from one dimer−dimer contact region have to propagate through the dimer to change the binding affinity of the second dimer-binding site. Helices of the intradimer interface are thereby crucial in facilitating these conformational changes (Figure 1). We hypothesize that oxidation of the free dimer constrains the intradimer interface. This constraint may lock Cp149 into an incorrect geometry or prevent it from adopting multiple geometries that play a role in assembly, a dynamic explanation. In agreement with this, we observe that Cp149ox slowly forms small amounts of capsids compared to the amount of capsids formed by Cp149red (Figures 2b and 3), though these appear to be identical to capsids formed by Cp149red (Figure 4b,c).

Thermodynamic analysis revealed a weaker pairwise dimer contact energy ($\Delta G_{contact}$) and strongly decreased values for the enthalpy (ΔH) and entropy (ΔS) for assembly of Cp149ox compared to those of Cp149red (Table 1). Because the final capsids have very similar structures, we propose that the greatest source of the entropy and enthalpy difference between Cp149red and Cp149ox arises from differences in the conformation of the inactive and active states. To a first approximation, the ΔH of assembly is related to the change in the amount of buried surface area, while ΔS correlates with the amount of replaced bulk water and the change in molecular degrees of freedom.[33] Given that the amount of buried surface in the capsid is approximately the same, the lower values for ΔH and ΔS suggest that Cp149ox free dimer has less exposed hydrophobic surface area and is more constrained (Table 1). The formation of higher proportions of T = 3 particles during assembly of Cp149ox compared to that of Cp149 suggests that Cp149ox has a slightly distorted geometry (Figure 4).

Assembly kinetic studies for Cp149ox also indicate that Cp149ox adopts unfavorable conformation(s) for capsid elongation. Cp149ox assembled 1.7 times slower than Cp149red, indicating a higher kinetic barrier to completing a capsid (Figures 5 and 7b). We propose that the slower elongation is due to intermediates that are more prone to dissociation. Over the course of the assembly reaction, dissociation of these intermediates contributes to a net decreased elongation rate.

Together, our data suggest that constraining the intradimer interface affects the thermodynamics and kinetics of assembly. Oxidized protein raises the barrier to the adoption of an assembly active conformation ($\Delta G^{\ddagger}_{activation}$) and weakens the dimer−dimer contact energy ($\Delta G_{con,ox}$), resulting in the slow formation of capsids that are less stable than those of Cp149red (Figure 7b).

These results strongly support the hypothesis that allosteric changes differentiate the stages of HBV assembly. We have shown that modulating the intradimer interface influences assembly kinetics and capsid stability. Our data imply that flexibility at the intradimer interface is beneficial for efficient capsid assembly. The dynamic nature of the core protein is also evident in the recently determined structure of HBeAg.[8] Expressed from the same RNA transcript, HBeAg comprises the core protein assembly domain with a 10-amino acid N-terminal extension, the remains of a signal sequence. Cysteine 61 of HBeAg can form a disulfide bond with cysteine −7 located in the N-terminal extension.[34] In HBeAg, the dimer interface is flipped by 140° to accommodate the C(−7)−C61 disulfide, indicating the feasibility of a substantial rearrangement of the intradimer interface.[8,25] Furthermore, the dynamic nature of the core protein is demonstrated by HDX−MS experiments. Deuterium exchange rates were bimodal for the C-terminal dimer−dimer contact region as well as the N-terminus, indicating that free dimer is more dynamic than dimers within capsids.[35] Also, emphasizing the importance of the intradimer interface in propagating allosteric changes are mutations such as F97L and L42A, located within and at the base of the spike tips, both of which alter capsid assembly (Figure 1).[29,36] Mutant F97L assembled faster than the wild-

dx.doi.org/10.1021/bi500732b | Biochemistry 2014, 53, 5496−5504

type protein, while mutation L42A completely abrogated assembly, despite being far from the dimer−dimer contact region.[29,36] These mutations illustrate the importance of the intradimer interface in propagating structural changes and facilitating the adoption of an assembly active conformation.

The poor stability of oxidized capsids estimated from assembly was consistent with urea disassembly. Capsids assembled from Cp149ox were less stable than capsids formed by Cp149-C61S, which mimics fully reduced capsid particles (Figure 6). These data indicate that reduced dimer is more suitable for capsid assembly than Cp149ox. One possible explanation for the enhanced stability of reduced capsids is that the dynamic interface allows reduced capsids to access more conformational states. Evidence of entropic stabilization has also been described for picornaviruses.[37−39]

Our findings also suggest a possible function for the C61−C61 disulfide. The mechanism underlying capsid disassembly at the nuclear membrane is still unclear. Our results indicate that oxidation could facilitate uncoating of the capsid particles. Increased internal capsid pressure due to genome maturation[40] together with capsid oxidation is predicted to lower the energy barrier to disassembly. Indeed, a recent study has shown that genome maturation in HBV virions is associated with a destabilization of the capsid, making it more sensitive to nuclease and protease treatment.[41] Consistently, C61−C61 disulfides have been observed in mature particles isolated from infected liver and cell cultures.[42−44]

C61 and the C61−C61 disulfide are not essential for assembly of core particles.[45,46] However, C61 is conserved in all mammalian hepadnaviruses. Our results show that the C61−C61 disulfide affects assembly, disassembly, and stability, indicating a physicochemical basis for its evolutionary conservation.

■ ASSOCIATED CONTENT

Supporting Information

Two figures showing the intrinsic fluorescence of Cp149 and Cp149-C61S during treatment with 0−3.8 M urea. This material is available free of charge via the Internet at http://pubs.acs.org.

■ AUTHOR INFORMATION

Corresponding Author

*Department of Molecular and Cellular Biochemistry, Indiana University, Bloomington, IN 47405. E-mail: azlotnic@indiana.edu. Phone: (812) 856-1925.

Present Address

§S.P.K.: Department of Pediatrics and Elizabeth B. Lamb Center for Pediatric Research, Vanderbilt University School of Medicine, Nashville, TN 37232-2581.

Funding

This work was supported by National Institutes of Health Grant R01-AI077688 to A.Z.

Notes

The authors declare no competing financial interest.

■ ACKNOWLEDGMENTS

We acknowledge Alex Kukreja for valuable comments about the manuscript and Joseph Che-Yen Wang for the graphic of the dimer structure included in the thermodynamic cycle.

■ ABBREVIATIONS

DTT, dithiothreitol; HBV, hepatitis B virus; HBeAg, hepatitis B virus e-antigen; SEC, size-exclusion chromatography; HDX−MS, hydrogen−deuterium exchange−mass spectrometry; SDS−PAGE, sodium dodecyl sulfate−polyacrylamide gel electrophoresis; HEPES, 4-(2-hydroxyethyl)-1-piperazineethanesulfonic acid; HPLC, high-performance liquid chromatography; TEM, transmission electron microscopy; K_{Dapp}, apparent dissociation constant; $K_{contact}$, pairwise dimer−dimer dissociation constant; f_{red}, elongation rate constant for reduced dimer; f_{ox}, elongation rate constant for oxidized dimer; $\Delta G_{contact}$, pairwise dimer−dimer contact energy; $\Delta G_{con,red}$, pairwise dimer−dimer contact energy for reduced dimer; $\Delta G_{con,ox}$, pairwise dimer−dimer contact energy for oxidized dimer; C_{red}, reduced capsid; C_{ox}, oxidized capsid; $\Delta G^{\ddagger}_{activation}$, activation energy of capsid assembly; ΔG_{S-S}, energy term including C61−C61 disulfide formation and dimer−dimer interactions.

■ REFERENCES

(1) Caspar, D. L. (1980) Movement and self-control in protein assemblies. Quasi-equivalence revisited. *Biophys. J. 32*, 103−138.

(2) Zlotnick, A., and Mukhopadhyay, S. (2011) Virus assembly, allostery and antivirals. *Trends Microbiol. 19*, 14−23.

(3) Packianathan, C., Katen, S. P., Dann, C. E., III, and Zlotnick, A. (2010) Conformational changes in the hepatitis B virus core protein are consistent with a role for allostery in virus assembly. *J. Virol. 84*, 1607−1615.

(4) Dykeman, E. C., Stockley, P. G., and Twarock, R. (2010) Dynamic allostery controls coat protein conformer switching during MS2 phage assembly. *J. Mol. Biol. 395*, 916−923.

(5) Taylor, G. M., Ma, L., Vogt, V. M., and Post, C. B. (2010) NMR relaxation studies of an RNA-binding segment of the rous sarcoma virus gag polyprotein in free and bound states: A model for autoinhibition of assembly. *Biochemistry 49*, 4006−4017.

(6) Stray, S. J., Ceres, P., and Zlotnick, A. (2004) Zinc ions trigger conformational change and oligomerization of hepatitis B virus capsid protein. *Biochemistry 43*, 9989−9998.

(7) Packianathan, C., Katen, S. P., Dann, C. E., III, and Zlotnick, A. (2009) Conformational changes in the hepatitis B virus core protein are consistent with a role for allostery in virus assembly. *J. Virol. 84*, 1607−1615.

(8) DiMattia, M. A., Watts, N. R., Stahl, S. J., Grimes, J. M., Steven, A. C., Stuart, D. I., and Wingfield, P. T. (2013) Antigenic switching of hepatitis B virus by alternative dimerization of the capsid protein. *Structure 21*, 133−142.

(9) Crowther, R. A., Kiselev, N. A., Bottcher, B., Berriman, J. A., Borisova, G. P., Ose, V., and Pumpens, P. (1994) Three-dimensional structure of hepatitis B virus core particles determined by electron cryomicroscopy. *Cell 77*, 943−950.

(10) Birnbaum, F., and Nassal, M. (1990) Hepatitis B virus nucleocapsid assembly: Primary structure requirements in the core protein. *J. Virol. 64*, 3319−3330.

(11) Wingfield, P. T., Stahl, S. J., Williams, R. W., and Steven, A. C. (1995) Hepatitis core antigen produced in *Escherichia coli*: Subunit composition, conformational analysis, and in vitro capsid assembly. *Biochemistry 34*, 4919−4932.

(12) Kenney, J. M., von Bonsdorff, C. H., Nassal, M., and Fuller, S. D. (1995) Evolutionary conservation in the hepatitis B virus core structure: Comparison of human and duck cores. *Structure 3*, 1009−1019.

(13) Zlotnick, A., Cheng, N., Conway, J. F., Booy, F. P., Steven, A. C., Stahl, S. J., and Wingfield, P. T. (1996) Dimorphism of hepatitis B virus capsids is strongly influenced by the C-terminus of the capsid protein. *Biochemistry 35*, 7412−7421.

(14) Zlotnick, A. (2005) Theoretical aspects of virus capsid assembly. *J. Mol. Recognit. 18*, 479−490.

(15) Hagan, M. F., and Chandler, D. (2006) Dynamic Pathways for Viral Capsid Assembly. *Biophys. J. 91*, 42−54.
(16) Katen, S. P., and Zlotnick, A. (2009) Thermodynamics of Virus Capsid Assembly. *Methods Enzymol. 455*, 395−417.
(17) Ceres, P., and Zlotnick, A. (2002) Weak protein-protein interactions are sufficient to drive assembly of hepatitis B virus capsids. *Biochemistry 41*, 11525−11531.
(18) Mohan, S., Kourentzi, K., Schick, K. A., Uehara, C., Lipschultz, C. A., Acchione, M., Desantis, M. E., Smith-Gill, S. J., and Willson, R. C. (2009) Association energetics of cross-reactive and specific antibodies. *Biochemistry 48*, 1390−1398.
(19) Zheng, J., Schodel, F., and Peterson, D. (1992) The structure of hepadnaviral core antigens. Identification of free thiols and determination of the disulfide bonding pattern. *J. Biol. Chem. 267*, 9422−9429.
(20) Gallina, A., Bonelli, F., Zentilin, L., Rindi, G., Muttini, M., and Milanesi, G. (1989) A recombinant hepatitis B core antigen polypeptide with the protamine-like domain deleted self-assembles into capsid particles but fails to bind nucleic acids. *J. Virol. 63*, 4645−4652.
(21) Yu, X., Jin, L., Jih, J., Shih, C., and Zhou, Z. H. (2013) 3.5Å cryoEM structure of hepatitis B virus core assembled from full-length core protein. *PLoS One 8*, e69729.
(22) Zlotnick, A., Ceres, P., Singh, S., and Johnson, J. M. (2002) A small molecule inhibits and misdirects assembly of hepatitis B virus capsids. *J. Virol. 76*, 4848−4854.
(23) Hagan, M. F., and Elrad, O. M. (2010) Understanding the concentration dependence of viral capsid assembly kinetics: The origin of the lag time and identifying the critical nucleus size. *Biophys. J. 98*, 1065−1074.
(24) Dirnhuber, P., and Schutz, F. (1948) The isomeric transformation of urea into ammonium cyanate in aqueous solutions. *Biochem. J. 42*, 628−632.
(25) Zlotnick, A., Tan, Z., and Selzer, L. (2013) One protein, at least three structures, and many functions. *Structure 21*, 6−8.
(26) Darby, N., and Creighton, T. E. (1997) Probing protein folding and stability using disulfide bonds. *Mol. Biotechnol. 7*, 57−77.
(27) Yuan, T. T., Tai, P. C., and Shih, C. (1999) Subtype-independent immature secretion and subtype-dependent replication deficiency of a highly frequent, naturally occurring mutation of human hepatitis B virus core antigen. *J. Virol. 73*, 10122−10128.
(28) Yuan, T. T., Sahu, G. K., Whitehead, W. E., Greenberg, R., and Shih, C. (1999) The mechanism of an immature secretion phenotype of a highly frequent naturally occurring missense mutation at codon 97 of human hepatitis B virus core antigen. *J. Virol. 73*, 5731−5740.
(29) Ceres, P., Stray, S. J., and Zlotnick, A. (2004) Hepatitis B Virus Capsid Assembly is Enhanced by Naturally Occurring Mutation F97L. *J. Virol. 78*, 9538−9543.
(30) Zlotnick, A. (2007) Distinguishing reversible from irreversible virus capsid assembly. *J. Mol. Biol. 366*, 14−18.
(31) Li, L., Chirapu, S. R., Finn, M. G., and Zlotnick, A. (2013) Phase diagrams map the properties of antiviral agents directed against hepatitis B virus core assembly. *Antimicrob. Agents Chemother. 57*, 1505−1508.
(32) Singh, S., and Zlotnick, A. (2003) Observed hysteresis of virus capsid disassembly is implicit in kinetic models of assembly. *J. Biol. Chem. 278*, 18249−18255.
(33) Tanford, C. (1980) *The Hydrophobic Effect: Formation of Micelles and Biological Membranes*, 2nd ed., John Wiley and Sons, Inc., New York.
(34) Nassal, M., and Rieger, A. (1993) An intramolecular disulfide bridge between Cys-7 and Cys-61 determines the structure of the secretory core gene product (e antigen) of hepatitis B virus. *J. Virol. 67*, 4307−4315.
(35) Bereszczak, J. Z., Watts, N. R., Wingfield, P. T., Steven, A. C., and Heck, A. J. (2014) Assessment of differences in the conformational flexibility of hepatitis B virus core-antigen and e-antigen by hydrogen deuterium exchange-mass spectrometry. *Protein Sci. 23*, 884−896.
(36) Alexander, C. G., Jurgens, M. C., Shepherd, D. A., Freund, S. M., Ashcroft, A. E., and Ferguson, N. (2013) Thermodynamic origins of protein folding, allostery, and capsid formation in the human hepatitis B virus core protein. *Proc. Natl. Acad. Sci. U.S.A. 110*, E2782−E2791.
(37) Phelps, D. K., and Post, C. B. (1995) A novel basis of capsid stabilization by antiviral compounds. *J. Mol. Biol. 254*, 544−551.
(38) Tsang, S. K., Danthi, P., Chow, M., and Hogle, J. M. (2000) Stabilization of poliovirus by capsid-binding antiviral drugs is due to entropic effects. *J. Mol. Biol. 296*, 335−340.
(39) Speelman, B., Brooks, B. R., and Post, C. B. (2001) Molecular dynamics simulations of human rhinovirus and an antiviral compound. *Biophys. J. 80*, 121−129.
(40) Dhason, M. S., Wang, J. C., Hagan, M. F., and Zlotnick, A. (2012) Differential assembly of hepatitis B virus core protein on single- and double-stranded nucleic acid suggest the dsDNA-filled core is spring-loaded. *Virology 430*, 20−29.
(41) Cui, X., Ludgate, L., Ning, X., and Hu, J. (2013) Maturation-associated destabilization of hepatitis B virus nucleocapsid. *J. Virol. 87*, 11494−11503.
(42) Budkowska, A., Shih, J. W., and Gerin, J. L. (1977) Immunochemistry and polypeptide composition of hepatitis B core antigen (HBc Ag). *J. Immunol. 118*, 1300−1305.
(43) Jeng, K. S., Hu, C. P., and Chang, C. M. (1991) Differential formation of disulfide linkages in the core antigen of extracellular and intracellular hepatitis B virus core particles. *J. Virol. 65*, 3924−3927.
(44) Hui, E. K., Yi, Y. S., and Lo, S. J. (1999) Hepatitis B viral core proteins with an N-terminal extension can assemble into core-like particles but cannot be enveloped. *J. Gen. Virol. 80* (Part 10), 2647−2659.
(45) Nassal, M. (1992) Conserved cysteines of the hepatitis B virus core protein are not required for assembly of replication-competent core particles nor for their envelopment. *Virology 190*, 499−505.
(46) Zhou, S., and Standring, D. N. (1992) Cys residues of the hepatitis B virus capsid protein are not essential for the assembly of viral core particles but can influence their stability. *J. Virol. 66*, 5393−5398.